

## Atomic and electronic structures of the two different layers in $4Hb$ -TaS<sub>2</sub> at 4.2 K

Inger Ekvall

*Department of Physics, Chalmers University of Technology and Göteborg University, SE-412 96 Göteborg, Sweden*

Ju-Jin Kim

*Department of Physics, Chalmers University of Technology and Göteborg University, SE-412 96 Göteborg, Sweden  
and Department of Physics, Chonbuk National University, Chonju 560-756, Korea*

Håkan Olin

*Department of Physics, Chalmers University of Technology and Göteborg University, SE-412 96 Göteborg, Sweden  
(Received 12 September 1996)*

We have studied the atomic and electronic structures of the two different layers in  $4Hb$ -TaS<sub>2</sub> prepared by a layer-by-layer etching technique using a scanning tunneling microscope at 4.2 K. One layer ( $1T$ ) showed the typical  $\sqrt{13} \times \sqrt{13}$  charge-density-wave structure, whereas the other layer ( $1H$ ) had at low bias a triangular atomic structure with weakly superposed  $3 \times 3$  and at high positive bias a  $\sqrt{13} \times \sqrt{13}$  charge-density-wave structure originating from the lower  $1T$  layer due to tunneling through the top  $1H$  layer. The bias-dependent-intensity of this charge-density-wave structure was shown to be consistent with room-temperature measurements, showing that this is a real intrinsic property of the material. Measured tunneling spectra of each layer at 4.2 K showed a metallic  $1H$  layer and an insulating  $1T$  layer with an opening of wide-gap structures at the Fermi level. [S0163-1829(97)03912-X]

The transition-metal dichalcogenides consist of sandwiches of one transition-metal atom (e.g., Ti, Ta, and Nb) between two chalcogen atoms (e.g., S, Se, and Te) and have been extensively studied by electron diffraction,<sup>1</sup> resistivity measurements,<sup>2-4</sup> and scanning tunneling microscopy (STM).<sup>5</sup> The two-dimensional structure of the transition-metal dichalcogenides cause charge-density waves (CDW's), standing waves of electron density, below a certain transition temperature. The formation of the CDW opens a gap at the Fermi level. In a strictly one-dimensional material the gap would lead to a metal-insulator transition, while in real materials the behavior need not be insulating. The transition-metal dichalcogenides exist in different types, depending on the coordination between the transition-metal atom and the chalcogen atoms. The  $T$  type has octahedral coordination between the transition-metal atom and the chalcogen atoms and the  $H$  type has trigonal prismatic coordination. The  $4Hb$  type consists of four alternating layers of  $1T$  and  $1H$  sandwiches (Fig. 1). This alternating-layer structure gives interesting atomic and electronic properties that were understood as a composite nature of those observed in the pure octahedral and trigonal prismatic types. Each layer is also believed to maintain its characteristic features found in the corresponding pure types, although there is a small electron transfer between the two different layers.<sup>6</sup>

Due to the weak van der Waals force between each layer in the transition-metal dichalcogenides, it is possible to etch away individual layers in a well-defined manner using STM.<sup>7,8</sup> Using this technique, it should be possible to choose different layers in the polytype transition-metal dichalcogenides by making new layers. This also enables one to study the atomic and electronic structures on the two different layers under exactly the same tunneling condition.

According to the scanning tunneling microscope studies by Giambattista *et al.*<sup>9</sup> and Coleman *et al.*,<sup>5</sup>  $4Hb$ -TaS<sub>2</sub> has completely different kinds of images on the two opposite faces of the same crystal cleave. One kind has a  $\sqrt{13} \times \sqrt{13}$  CDW and the other kind has atomic structures, presumably representing the  $1T$ -type and  $1H$ -type layers. Han *et al.*<sup>10</sup> observe strong bias-dependent STM images at room temperature. A fully developed  $\sqrt{13} \times \sqrt{13}$  CDW is observed even on the presumably  $1H$  surface at a relatively high positive bias voltage. Therefore, it is very important to identify each layer precisely, that is, whether the top layer is  $1T$  or  $1H$ .

Recently, a STM study of  $4Hb$ -TaS<sub>2</sub> was performed by Kim and Olin<sup>11</sup> at room temperature and at 77 K. In this study the layer-by-layer etching technique is used to make well-defined steps of alternating  $1T$  and  $1H$  layers that can be imaged simultaneously with exactly the same tunneling conditions. The STM images of  $1T$  layers show a strong  $\sqrt{13} \times \sqrt{13}$  CDW superlattice regardless of the bias voltage. The  $1H$  layers show a triangular atomic lattice at negative bias voltages and a weak  $\sqrt{13} \times \sqrt{13}$  CDW superlattice at high positive bias voltages, consistent with the measurements of Han *et al.*<sup>10</sup> No CDW arises in the  $1H$  layer at these temperatures since the CDW onset in the  $4Hb$ -TaS<sub>2</sub> is at 22 K, which is much lower than in the pure  $2H$ -TaS<sub>2</sub>, which has an onset temperature of 75 K. Tunneling spectra at the different layers show metallic  $1H$  layers and insulating  $1T$  layers, giving an alternating stack of insulating and conducting layers, which have been proposed earlier.<sup>2</sup> However, thermal fluctuations, tunneling between layers, and low-energy resolution could modify the spectra at higher temperatures. A study at 4.2 K would reveal not only discrepan-

cies in the spectra, but also the  $3\times 3$  CDW in the  $1H$  layer and the bias dependence of the  $\sqrt{13}\times\sqrt{13}$  CDW in the  $1H$  layer originating from the underlying  $1T$  layer. The layer-by-layer technique ensures that the two different layers are imaged under exactly the same tunneling conditions.

In this study, we have fabricated steps of  $4Hb$ -TaS<sub>2</sub> with height  $\sim 6$  Å by the layer-by-layer etching technique and investigated the electronic and atomic structures on the two different layers near the step region at 4.2 K. The measured STM images and tunneling spectra revealed completely different atomic and electronic structures of the  $1T$ - and  $1H$ -type layers. The  $1T$ -type layers showed the typical  $\sqrt{13}\times\sqrt{13}$  CDW structures, whereas the  $1H$ -type layers had the triangular atomic structure with a weak  $3\times 3$  CDW superlattice at negative and low positive bias voltages and a superposed  $\sqrt{13}\times\sqrt{13}$  CDW superlattice at a high positive bias voltage. We quantitatively estimated the bias-dependent intensity of these superposed CDW and found results quite consistent with those of Han *et al.*,<sup>10</sup> showing that this dependence is a pure intrinsic property and not a thermal effect. The measured tunneling spectra on each layer at 4.2 K also showed entirely different characteristics between the two layers near the step. The  $1H$  layer showed a metallic behavior, whereas the  $1T$  layer showed a wide insulating gap structure at the Fermi level at 4.2 K, more pronounced than at 77 K.

Single crystals of  $4Hb$ -TaS<sub>2</sub> were grown by the usual iodine transport method. The samples were cleaved at room temperature in air and set in the STM unit, which was placed in the center of a doubly shielded cryostat in a He exchange gas environment. The STM unit was cooled very slowly to 4.2 K for low-temperature experiments. Mechanically polished Pt/Ir tips were used. All images were obtained in the constant current mode. The sign of the bias voltage corresponds to sample voltage.

Figure 1 shows a summary view of a  $445\times 445$  Å<sup>2</sup> area of the  $4Hb$ -TaS<sub>2</sub> single crystal at 4.2 K exhibiting a step structure. The tunneling current and bias voltage were 5 nA and 100 mV, respectively. Originally, this area consisted of a surface with a strong modulation of  $\sqrt{13}\times\sqrt{13}$  CDW superlattice presumably corresponding to the  $1T$  phase. By scanning continuously with a relatively small tunneling resistance on the specified area, we could remove part of the layer as shown in Fig. 1 using the layer-by-layer etching method and image the two different layers at the same time. The step height was estimated to about 6 Å, which is equivalent to the lattice constant along the  $c$  axis within experimental error. It shows that the step is made up of one S-Ta-S molecular layer.<sup>1,5</sup> This kind of etching method allows us to clearly distinguish between the two types of layers that exist. STM images near a boundary region show clearly two regions separated by a step. The upper layer in Fig. 1 shows a strong modulation with a periodicity  $\sim 12$  Å, that is, the  $\sqrt{13}\times\sqrt{13}$  CDW superlattice corresponding to the  $1T$  layer. A rather flat surface exhibiting an atomic structure with a lattice constant  $\sim 3$  Å, believed to be the  $1H$  layer, is seen in the lower layer.

To study the more detailed structures, we measured STM images with a small scan area on the surface of two different layers. The STM image of the upper layer in Fig. 1 shows

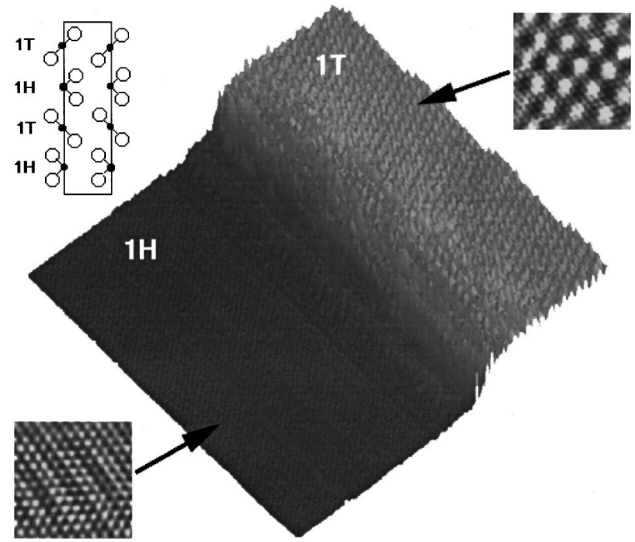


FIG. 1. Summary view of  $4Hb$ -TaS<sub>2</sub>. The two different layers show different images. Step image: sample bias voltage 100 mV and tunneling current 5 nA. Image size,  $445\times 445$  Å<sup>2</sup>. Small images: sample bias voltage 500 mV and tunneling current 1 nA (upper layer); sample bias voltage  $-50$  mV and tunneling current 1 nA (lower layer). Image size  $34\times 34$  Å<sup>2</sup>. Also shown is a schematic of the crystal structure of  $4Hb$ -TaS<sub>2</sub>.

the typical  $\sqrt{13}\times\sqrt{13}$  CDW modulation with a  $z$  modulation  $\sim 1.2$  Å at a bias voltage of 500 mV, with small atomic modulations. At low bias voltage, we observed only the strong  $\sqrt{13}\times\sqrt{13}$  CDW modulation with a large  $z$  deflection  $\sim 3.5$  Å. Although the amplitude of the CDW modulation decreased with increasing bias voltage, we could observe  $\sqrt{13}\times\sqrt{13}$  CDW structures in this layer over the whole voltage region measured (up to 500 mV). In the lower layer we obtained strong bias-dependent images. At bias voltages below  $+50$  mV, we observed a very weak  $3\times 3$  CDW superlattice [Fig. 2(a)]. The much lower CDW onset temperature of the  $1H$  layer in  $4Hb$ -TaS<sub>2</sub> ( $\sim 22$  K) than that of the corresponding pure phase ( $\sim 75$  K) (Refs. 3 and 12) makes this  $3\times 3$  structure difficult to see. Only weak structures, compared to the pure  $2H$  type, have been observed.<sup>5</sup> At a relatively high positive bias voltage, larger than  $\sim 200$  mV, we observed a completely different kind of CDW pattern, that is,

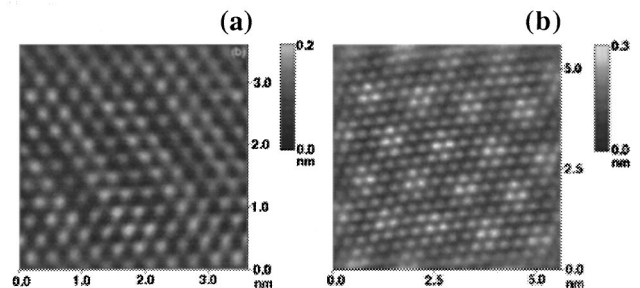


FIG. 2. (a) STM image on the lower layer in Fig. 1 with a bias voltage  $-50$  mV, showing a very weak  $3\times 3$  CDW. (b) STM image on the lower layer in Fig. 1 with a high positive bias voltage of 300 mV, showing the  $\sqrt{13}\times\sqrt{13}$  CDW originating from the underlying  $1T$  layer.

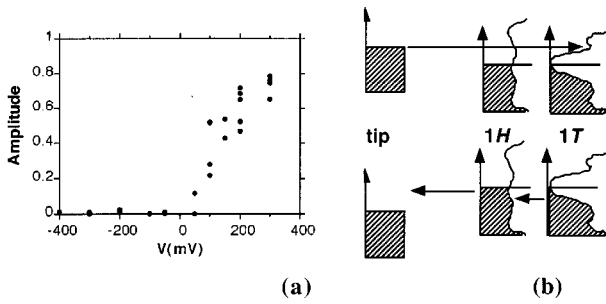


FIG. 3. (a) Intensity of  $\sqrt{13} \times \sqrt{13}$  CDW modulation in the 1H layer as a function of bias voltage at 4.2 K. (b) Schematic of the density of states in 1H and 1T layers. Positively biased electrons can tunnel through the 1H layer into the unoccupied states in the 1T layer, while negatively biased electrons will tunnel only from the overlying 1H layer because of the barrier the filled states cause.

a  $\sqrt{13} \times \sqrt{13}$  CDW modulation that arises from the second 1T layer [Fig. 2(b)] with the clear surface  $S$  atomic structures resolved. The atomic structures in the  $\sqrt{13} \times \sqrt{13}$  CDW in the 1H layer were much clearer than those in the 1T layer. Figure 3(a) shows the intensity of the  $\sqrt{13} \times \sqrt{13}$  CDW modulation in the 1H layer as a function of bias voltage at 4.2 K. The CDW intensity was estimated from the corresponding spot in the Fourier transform of the STM image. For negative bias voltages, there are no appreciable  $\sqrt{13} \times \sqrt{13}$  CDW spot. As the bias increases from zero to positive bias,  $\sqrt{13} \times \sqrt{13}$  CDW modulation starts to appear around 50 mV and increases in amplitude with increasing bias voltage. This kind of bias-dependent STM image has also been observed at room temperature in this material by Han *et al.*<sup>10</sup> and is explained in terms of an energy-dependent tunneling process between 1T and 1H layers. Comparing our low-temperature results with the room-temperature data of Han *et al.*, they show almost the same characteristics. This means that the bias dependence of the STM image should be related to the difference in the intrinsic band structures of the two different layers and not to temperature effects. Our CDW amplitude is somewhat smaller than the one observed by Han *et al.*, probably due to smaller interaction between the different layers in our sample. The energy dependence has been explained as tunneling from the 1T layer through the overlying 1H layer. The 1T layer has a gap due to the CDW transition, as shown in the spectra in Fig. 4(a). However, the

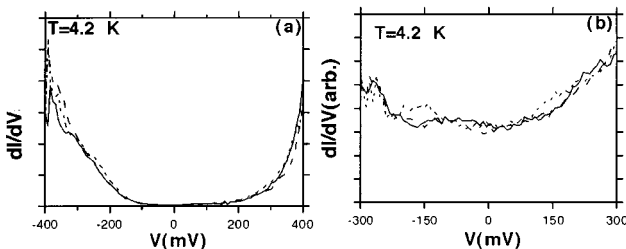


FIG. 4. Tunneling spectra at 4.2 K of the (a) 1T layer showing an insulating gap structure and (b) 1H layer showing that this layer is metallic.

1H layer remains metallic below the CDW transition, which can be seen in Fig. 4(b). A schematic of the two different layers is shown in Fig. 3(b). Tunneling from the 1T layer is suppressed at negative bias because of the barrier caused by the occupied states in the 1H layer. At positive bias electrons can tunnel through the unoccupied states in the 1H layer to the underlying unoccupied 1T layer states giving a  $\sqrt{13} \times \sqrt{13}$  CDW image even in the 1H layer. A similar effect has been observed in bias-dependent STM images of the high- $T_c$  superconductor  $\text{Bi}_2\text{Sr}_2\text{CaCu}_2\text{O}_{8+\delta}$ .<sup>13,14</sup> Tunneling from the metallic Cu-O plane is seen through the insulating Sr-O plane and the semiconducting Bi-O plane when the applied bias voltage is smaller than the energy gap in the Bi-O layer. The interlayer distance between the Bi-O plane and the Cu-O plane is of the same order as the interlayer distance in our sample, i.e., about 6–7 Å.

A resistivity measurement by Wattaniuk, Tidman, and Frindt<sup>2</sup> shows that the polytype 4Hb-TaS<sub>2</sub> has different conductivity along and across the layer. Metallic conductivity was observed along the layers, with an insulating behavior perpendicular the layers, suggesting a stack of alternating metallic and insulating layers. From analogies in the electrical properties of the corresponding pure phases 2H-TaS<sub>2</sub>, which is metallic along the layer, and 1T-TaS<sub>2</sub>, which is insulating along the layer, they assume that 1T layer would be insulating and 1H would be metallic.

Tanaka *et al.*<sup>15,16</sup> tried to distinguish 1T from 1H layers with tunneling spectra and obtained characteristic ones corresponding to the 1H- and 1T-type layers at room temperature. However, the observed tunneling spectra at room temperature are too obscure to distinguish each layer precisely due to large thermal fluctuations and inter-layer tunneling effects. Coleman *et al.*<sup>12</sup> also measured the tunneling spectra on an unspecified layer in this compound at 4.2 K. Their results show quite interesting gap structures, which consist of several sharp peak structures related to the harmonics of the 1T gap. They pointed out that this may arise from stacks consisting of the insulating 1T layer and metallic 1H layer. To avoid this kind multiple-tunnel-junction effect across the barriers made up of the alternating 1T and 1H layers, we made the electrical contacts around the rim of the whole sample except on the top layer in the scanning region. This gives smaller interaction and is probably the reason for our lower CDW amplitudes compared to those of Han *et al.* New layers were made by the layer-by-layer etching method and the tunneling spectra were measured at different layers separately. Our tunneling spectra on each layer show a stack of metallic 1H and insulating 1T directly and clearly. The gap in the 1T layer is wider and clearer than in the 77 K study.<sup>11</sup>

In summary, we have investigated the electronic and atomic structures at 4.2 K on the two different layers of 1T and 1H type in 4Hb-TaS<sub>2</sub> near a step region prepared by the layer-by-layer etching technique. The measured STM images and tunneling spectra revealed completely different atomic and electronic structures of the 1T- and 1H-type layers. The 1T-type layers showed the typical  $\sqrt{13} \times \sqrt{13}$  CDW structures, whereas the 1H-type layers had a triangular atomic structure with a weak  $3 \times 3$  CDW superlattice at negative and low positive bias voltage and a superposed  $\sqrt{13} \times \sqrt{13}$  CDW superlattice at high positive bias voltage. The bias-dependent CDW intensity was consistent with the room-temperature in-

tensity reported earlier<sup>10</sup> showing that this is a real intrinsic property of the material and not a thermal effect. The measured tunneling spectra on each layer at 4.2 K also showed entirely different electronic structures between the two layers near the step. The  $1H$  layer showed a metallic behavior, whereas the  $1T$  layer showed an opening of a wide insulating gap at the Fermi level. This gives two ways of determining

which layer is the top layer in  $4Hb$ -TaS<sub>2</sub>: by STM images at negative and low positive bias voltage and by spectroscopy.

This work was supported by the Swedish Research Council for Engineering Science (TFR). We would like to thank Dr. Hans Starnberg and Professor F. Levy for providing us with the single crystals.

- 
- <sup>1</sup>J. A. Wilson, F. J. DiSalvo, and S. Mahasan, *Adv. Phys.* **24**, 117 (1975).
- <sup>2</sup>W. J. Wattamaniuk, J. P. Tidman, and R. F. Frindt, *Phys. Rev. Lett.* **35**, 62 (1975).
- <sup>3</sup>R. H. Friend, D. Jerome, R. F. Frindt, and A. J. Yoffe, *J. Phys. C* **10**, 1013 (1977).
- <sup>4</sup>F. J. DiSalvo, B. J. Bagley, J. M. Voorhoeve, and J. V. Waszczak, *J. Phys. Chem. Solids* **34**, 1357 (1973).
- <sup>5</sup>R. V. Coleman, B. Giambattista, P. K. Hansma, A. Johnson, W. W. McNairy, and C. G. Slough, *Adv. Phys.* **37**, 559 (1988).
- <sup>6</sup>N. J. Doran, G. Wexler, and A. M. Woolley, *J. Phys. C* **11**, 2967 (1978).
- <sup>7</sup>B. Parkinson, *J. Am. Chem. Soc.* **112**, 7498 (1990).
- <sup>8</sup>A. P. Volodin and J. Aarts, *Physica C* **235**, 1909 (1994).
- <sup>9</sup>B. Giambattista, A. Johnson, W. W. McNairy, C. G. Slough, and R. V. Coleman, *Phys. Rev. B* **38**, 3545 (1988).
- <sup>10</sup>W. H. Han, E. R. Hunt, O. Pankratov, and R. F. Frindt, *Phys. Rev. B* **50**, 14 746 (1994).
- <sup>11</sup>J.-J. Kim and H. Olin, *Phys. Rev. B* **52**, R14 388 (1995).
- <sup>12</sup>R. V. Coleman, Z. Dai, W. W. McNairy, C. G. Slough, and C. Wang, in *Scanning Tunneling Microscopy*, edited by J. A. Stroscio and W. J. Kaiser (Academic, San Diego, 1993).
- <sup>13</sup>C. Manabe, M. Oda, and M. Ido, *Physica C* **235**, 797 (1994).
- <sup>14</sup>M. Oda, C. Manabe, and M. Ido, *Phys. Rev. B* **53**, 2253 (1996).
- <sup>15</sup>M. Tanaka, S. Yamazaki, K. Kajimura, H. Bando, T. Nakashizu, N. Morita, W. Mizutani, and M. Ono, *J. Microsc.* **152**, 183 (1988).
- <sup>16</sup>M. Tanaka, H. Tokumoto, T. Nakashizu, W. Mizutani, K. Kajimura, S. Yamazaki, M. Ono, and H. Bando, *Jpn. J. Appl. Phys.* **28**, 473 (1989).